114

High Parton Density QCD.

3

Energy evolution and leading logarithm-$1/x$ approximation in QCD

We now begin the presentation of our main subject: high energy QCD, also known as small-x physics. We argue that at small Bjorken x it is natural to try to resum leading logarithms of $1/x$, that is, powers of $\alpha_s \ln 1/x$. Resummation of this parameter in the linear approximation corresponding to low parton density is accomplished by the Balitsky–Fadin–Kuraev–Lipatov (BFKL) evolution equation, which we describe in this chapter using the standard approach based on Feynman diagrams. Note that our derivation of the BFKL equation in this chapter is rather introductory in nature; a more rigorous re-derivation employing LCPT is left until for the next chapter. We point out some problems with the linear BFKL evolution; in particular we argue that it violates unitarity constraints for the scattering cross section. We describe initial attempts to solve the BFKL unitarity problem by introducing nonlinear corrections to the BFKL evolution, resulting in the Gribov–Levin–Ryskin and Mueller–Qiu (GLR–MQ) evolution equation. We discuss properties of the GLR–MQ evolution equation and, for the first time, introduce the saturation scale Q_s.

3.1 Paradigm shift

Our goal in this book is to study the high energy behavior of QCD. In the context of DIS the high energy asymptotics can be explored by fixing the photon virtuality Q^2 and taking the photon–proton center-of-mass energy $\hat{s}$ to be large. In this limit the Bjorken-x variable becomes small, as follows from Eq. (2.6). The small-x asymptotics is therefore synonymous with the high energy limit of QCD:

$$\text{small } x \Longleftrightarrow \text{high energy } s. \tag{3.1}$$

The small-x asymptotics of the gluon distribution function $xG(x, Q^2)$ in the framework of DGLAP evolution was discussed in Section 2.4.6. For the LLA DGLAP, the small-x asymptotics corresponds to summation of the parameter

$$\alpha_s \ln \frac{1}{x} \ln \frac{Q^2}{Q_0^2}, \tag{3.2}$$

which constitutes the double logarithm approximation (DLA). While in Sec. 2.4.6 we worked out the running coupling case, the small-x asymptotics of the gluon distribution function for fixed coupling can be shown to be that in Eq. (2.159). The resulting gluon

Table 3.1. *The transverse and longitudinal leading logarithmic approximations (LLAs) with for comparison the double logarithmic approximation (DLA)*

Approximation	Coupling	Transverse logarithm	Longitudinal logarithm
LLA in Q^2	$\alpha_s(Q^2) \ll 1$	$\alpha_s \ln(Q^2/Q_0^2) \approx 1$	$\alpha_s \ln 1/x \ll 1$
LLA in $1/x$	$\alpha_s \ll 1$	$\alpha_s \ln(Q^2/Q_0^2) \ll 1$	$\alpha_s \ln 1/x \approx 1$
DLA	$\alpha_s(Q^2) \ll 1$	$\alpha_s \ln(Q^2/Q_0^2) \ll 1$	$\alpha_s \ln 1/x \ll 1$
		but $\alpha_s \ln(Q^2/Q_0^2) \ln 1/x \approx 1$	

distribution grows with decreasing x in such a way that

$$\left(\frac{1}{x}\right)^a \gg xG(x, Q^2) \propto \exp\left(2\sqrt{\frac{\alpha_s N_c}{\pi} \ln\frac{1}{x} \ln\frac{Q^2}{Q_0^2}}\right) \gg \ln^n \frac{1}{x}, \tag{3.3}$$

which is faster than any positive power n of $\ln 1/x$ but slower than any positive power a of $1/x$.

The asymptotics of the gluon distribution (3.3) is valid in the double logarithmic limit of small x and large Q^2. However, if one is interested in studying the high energy (Regge) limit of QCD, one simply needs to fix Q^2 at some, not necessarily large, value and study the small-x asymptotics. As there is no need to take the large-Q^2 limit, $\ln(Q^2/Q_0^2)$ is now neither a large nor a small parameter. We therefore drop it from Eq. (3.2) and aim to resum the parameter

$$\alpha_s \ln\frac{1}{x}. \tag{3.4}$$

Resummation of a series in powers of the parameter (3.4) is referred to as the leading-logarithmic approximation (LLA) in $1/x$. As with previous logarithmic approximations we assume that the relevant transverse momentum scales are large enough that $\alpha_s \ll 1$. At small x we have $\ln 1/x \gg 1$, so that $\alpha_s \ln 1/x \sim 1$ and is an important parameter to resum. (Indeed, as we have seen from Sec. 2.4.6 already, and as will be clear from the calculations below, for gluon distribution functions and for total hadronic scattering cross sections one can have at most one power of $\ln 1/x$ per power of the coupling α_s, i.e., there is no resummation parameter like $\alpha_s \ln^2 1/x$ in xG though there are other observables, such as $\Delta^{f\bar{f}}$, which depend on this parameter: however, these are suppressed at high energy and the presentation of their low-x asymptotics is beyond the scope of this book.) As we will see in the next chapter, the resummation of gluon emissions in the light cone wave function presented in Sec. 2.4.2 can also be done in the LLA in $1/x$ instead of the LLA in Q^2, as used for DGLAP evolution.

Table 3.1 gives for comparison the two leading logarithmic approximations, that in Q^2 of Eq. (2.67) leading to the DGLAP equations and the other from Eq. (3.4) that we will study below. As discussed in Sec. 2.3, the photon virtuality Q determines the transverse size resolution of a DIS experiment, while Bjorken x determines the longitudinal (Ioffe) lifetime

of the partonic fluctuation: we therefore refer to $\ln Q^2$ as the transverse logarithm and to $\ln 1/x$ as the longitudinal logarithm. As one can see from Table 3.1, the two LLA regimes should give identical results when they overlap in the double logarithmic approximation (DLA).

As discussed in the previous chapter, the LLA in Q^2 leads to the evolution described by the DGLAP equations, which allows us to determine the number of partons with transverse size larger than $1/Q$ if we know the number of partons with size larger than $1/Q_0$. Formally speaking, Q_0 is chosen to be large enough that $\alpha_s(Q_0^2) \ll 1$. In x-evolution we hope to find the number of partons of roughly the same transverse size at low x if we know this number at some $x = x_0$. Therefore Fig. 2.22 would have to be modified for small-x evolution. We will return to this subject later, after deriving the linear small-x evolution equation.

Resummation of the leading logarithms of $1/x$ instead of those of Q^2 is the essential paradigm shift needed in studying the small-x asymptotics. The equation resumming leading logarithms of $1/x$ will be, unlike the DGLAP equation, an evolution equation in x not an evolution equation in Q^2. A main goal of this chapter is to develop the technique of summing such longitudinal logarithmic contributions. We will show that the summation of powers of $\alpha_s \ln 1/x$ leads to gluon distributions increasing as a power of $1/x$ at small x, namely as $(1/x)^{1+\text{const}\,\alpha_s}$. For hadron–hadron scattering cross sections, $\ln 1/x$ is replaced by $\ln s$ (cut off by some dimensionful scale), so that the resummation of longitudinal logarithms gives cross sections growing as a power of the center-of-mass energy: $\sigma_{tot} \sim s^{1+\text{const}\,\alpha_s}$.

3.2 Two-gluon exchange: the Low–Nussinov pomeron

We start our analysis of high energy scattering with the lowest-order diagrams. As mentioned earlier, in this chapter we will be using the usual Feynman diagram technique. For simplicity let us consider the high energy scattering of two quark–antiquark bound states (quarkonia) on each other. We assume that the quarkonia either resulted from a splitting of virtual photons of high virtuality Q ($\gamma^* + \gamma^*$ scattering) or consist of quarks sufficiently heavy to insure the applicability of perturbative QCD methods.

Before we start the calculation let us formulate a general rule for high energy scattering, which will be confirmed by explicit calculations below, albeit for the particular case of gluons. Consider high energy scattering event in which a particle of spin j is exchanged in the t-channel between some scatterers, as shown in Fig. 3.1. The rule is simple: if one wants to count the powers of the center-of-mass energy s in the total scattering cross section then the contribution of each t-channel exchange of particle with spin j to the scattering cross section is (Regge 1959, 1960)[1]

$$s^{j-1}. \tag{3.5}$$

To avoid confusion between contributions to the scattering amplitude and to the cross section we note that in our (standard) normalization the cross section is $\sigma \sim |M|^2/s^2$, where

[1] This simple rule applies only to counting powers of s and cannot be used to count the powers of $\ln s$, which is a much slower function of s than a power and is therefore neglected by the rule.

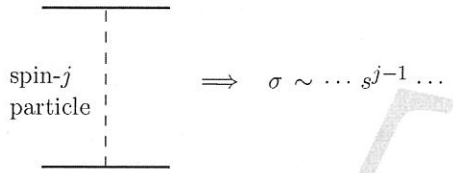

Fig. 3.1. A t-channel exchange of a particle with spin j between two particles scattering at high energy. The exchange shown is assumed to be part of some amplitude squared contributing to the scattering cross section. The contribution of each particle exchange to the resulting scattering cross section is s^{j-1}.

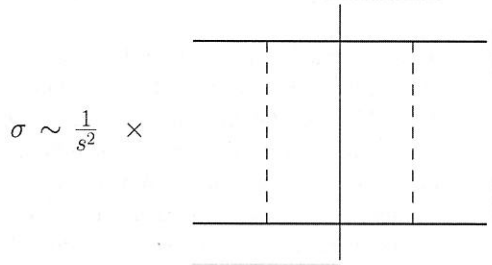

Fig. 3.2. The scattering cross section as the amplitude squared of the t-channel exchange diagram from Fig. 3.1 divided by the appropriate kinematic factors, including s^2. The vertical solid line denotes the final-state cut.

M is the scattering amplitude (see e.g. Amsler *et al.* (2008)). An exchange of k particles of spin j in the amplitude and k particles in the complex conjugate amplitude leads to a cross section scaling as $\sigma \sim s^{(j-1)2k}$, while the amplitude with k exchanged particles would then scale as $M \sim s^{1+(j-1)k}$. Hence one-particle exchange contributes s^j to the amplitude ($k = 1$), while the exchange of two particles ($k = 2$) gives a factor s^{2j-1} in the amplitude, etc.

As an example, consider the contribution of the squared amplitude in Fig. 3.1 to the total scattering cross section, as shown in Fig. 3.2. According to the above rule the cross section receives contributions from the exchanges of two t-channel particles of spin j, each contributing s^{j-1}. The resulting scattering cross section scales as

$$\sigma \sim s^{2(j-1)}. \tag{3.6}$$

Thus, if the particles exchanged in the t-channel were gluons with spin $j = 1$, the cross section would scale as

$$\sigma_{gluons} \sim s^0. \tag{3.7}$$

On the basis of rule (3.6) we would expect the cross section due to a two-gluon exchange to be constant with energy. This is an important observation, which we will soon verify by explicit calculations.

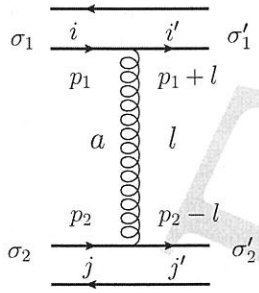

Fig. 3.3. Onium–onium high energy scattering amplitude at leading order. The arrows on the quark lines denote the directions of both the particle number flow and the momentum flow.

Alternatively, if the particles exchanged in the t-channel in Fig. 3.2 were quarks with spin $j = 1/2$ then the cross section would scale as

$$\sigma_{quarks} \sim \frac{1}{s} \tag{3.8}$$

and would decrease with energy. We see that, according to the above rule, the gluon contribution to the scattering cross section dominates the quark contribution. This conclusion is certainly in line with our earlier observation in Sec. 2.4.6 that the gluon distribution dominates in DIS at small x. We see that in high energy processes gluons play a more important role than quarks.

Let us consider the case when scalar particles are exchanged in the t-channel of Fig. 3.2 (we are now going beyond QCD and are considering a scalar theory). The cross section would scale as

$$\sigma_{scalars} \sim \frac{1}{s^2} \tag{3.9}$$

and is also, like the cross section for quark exchanges, small at high energy.

Finally, if spin-2 particles, such as gravitons, are exchanged in the t-channel of Fig. 3.2 then one gets

$$\sigma_{gravitons} \sim s^2 \tag{3.10}$$

and the cross section would grow rather fast with energy. Luckily, despite this energy enhancement, gravity is rather weakly coupled at the energies of modern-day accelerators and does not contribute significantly to the total cross sections.

Let us now return to QCD and to the high energy scattering of two quarkonia (to which we will often simply refer to as "onia"). In view of the above rule, and as can be shown by a simple calculation, at high energy the dominant lowest-order contribution to the QCD scattering amplitude is due to a t-channel gluon exchange, as shown in Fig. 3.3.

We are working in the center-of-mass frame, where the top onium (along with its quark and antiquark) in Fig. 3.3 has a large plus light cone component of momentum, while

the lower onium has a large minus momentum component. Specifically, for simplicity neglecting the quark masses one may choose the incoming quarks in Fig. 3.3 to be light-like:

$$p_1^\mu = (p_1^+ \equiv P^+ = \sqrt{s}, 0, 0_\perp) \quad \text{and} \quad p_2^\mu = (0, p_2^- \equiv P^- = \sqrt{s}, 0_\perp), \tag{3.11}$$

using the $(+, -, \perp)$ notation. Note that, in our high energy kinematics, P^+ and P^- are the two largest momentum scales in the problem; all other momenta are assumed to be much smaller than P^+ and P^-. This is known as the *eikonal approximation.*

A simple calculation in the covariant (Feynman) gauge yields the amplitude for the diagram in Fig. 3.3:

$$iM^0_{qq\to qq} = -ig^2 (t^a)_{i'i} (t^a)_{j'j} \frac{1}{l_\perp^2} \bar{u}_{\sigma_1'}(p_1 + l)\gamma^\mu u_{\sigma_1}(p_1) \bar{u}_{\sigma_2'}(p_2 - l)\gamma_\mu u_{\sigma_2}(p_2). \tag{3.12}$$

In arriving at Eq. (3.12) we have used the fact that the outgoing quarks are on mass shell, so that

$$0 = (p_1 + l)^2 = p_1^+ l^- + l^2, \tag{3.13}$$

giving

$$l^- = -\frac{l^2}{p_1^+} = -\frac{l^2}{P^+} \approx 0. \tag{3.14}$$

Similarly

$$l^+ = \frac{l^2}{p_2^-} = \frac{l^2}{P^-} \approx 0 \tag{3.15}$$

and, therefore,

$$l^2 \approx -l_\perp^2. \tag{3.16}$$

We see that in the high energy approximation the exchanged gluon has no longitudinal momentum: we will refer to it as an instantaneous or Coulomb gluon.

To keep only leading powers of P^+ and P^- we use the following trick: we consider that the spinors of the quark line with the large plus momentum (the upper line in Fig. 3.3) are chosen in the Lepage and Brodsky (1980) convention while the spinors in the quark line with the large minus momentum (the lower line in Fig. 3.3) are also chosen in the Lepage and Brodsky (1980) convention but with the P^- and P^+ momenta interchanged (see Eqs. (1.50) and (1.51)). Using Table A.1 in Appendix A we see that γ^+ dominates in the upper quark line of Fig. 3.3 since it carries a large P^+ momentum while γ^- dominates in the lower quark line, which carries a large P^- momentum. With the help of Table A.1 we then obtain[2]

$$M^0_{qq\to qq}(\vec{l}_\perp) = -2g^2 (t^a)_{i'i} (t^a)_{j'j} \delta_{\sigma_1\sigma_1'} \delta_{\sigma_2\sigma_2'} \frac{s}{l_\perp^2}. \tag{3.17}$$

[2] One may also use standard notation for Dirac spinors (see e.g Peskin and Schroeder (1995)). In this case, neglecting l compared to p_1 and p_2, one should use the relation $\bar{u}_{\sigma'}(p)\gamma^\mu u_\sigma(p) = 2p^\mu \delta_{\sigma\sigma'}$, which follows from the Gordon identity, to simplify Eq. (3.12).

The square of the amplitude in Eq. (3.17) leads to the following high energy cross section:

$$\sigma^0_{qq\to qq} = \frac{2\alpha_s^2 C_F}{N_c} \int \frac{d^2 l_\perp}{(l_\perp^2)^2}. \tag{3.18}$$

We see that, in agreement with the rule in Eq. (3.6), the cross section due to two t-channel gluon exchanges is independent of energy at high energy. This feature of QCD was first noticed by Low (1975) and Nussinov (1976). The two t-channel gluon exchange cross section is sometimes called the *Low–Nussinov pomeron*, since this result was the first successful attempt to describe hadronic cross sections in the framework of perturbative QCD: in pre-QCD language hadronic cross sections were described as being due to the t-channel exchange of a hypothetical particle with the quantum numbers of the vacuum called *the pomeron*, named after I. Y. Pomeranchuk (1958). The contribution of the pomeron to the scattering amplitude is

$$M \sim s^{\alpha(t)}, \tag{3.19}$$

where s and t are Mandelstam variables and $\alpha(t)$ is the "angular momentum" of the pomeron, usually referred to as the *pomeron trajectory*. The contribution of a single pomeron exchange to the total cross section is

$$\sigma_{tot} \sim s^{\alpha(0)-1}. \tag{3.20}$$

Here $\alpha(0)$ is the value of the pomeron trajectory at $t = 0$, which is the point where it intercepts the angular momentum axis in the (t, α)-plane. Therefore $\alpha(0)$ is referred to as the *pomeron intercept* and is sometimes denoted by α_P. As one can see from Eq. (3.20), the pomeron intercept always comes in the combination $\alpha(0) - 1$: according to a common notation, we will often refer to $\alpha(0) - 1 = \alpha_P - 1$ as itself the pomeron intercept. Frequently one uses a linear expansion of the pomeron trajectory near $t = 0$:

$$\alpha(t) \approx \alpha(0) + \alpha' t. \tag{3.21}$$

The parameter α' is called the *slope* of the pomeron trajectory. A tantalizing feature of strong interactions is that the linear approximation (3.21) actually describes the pomeron trajectory $\alpha(t)$ rather well at all values of t. This observation gave rise to the development of string theory, which started out as a candidate theory for strong interactions (see e.g. Green, Schwarz, and Witten (1987)).

From Eq. (3.18) it is clear that the Low–Nussinov pomeron has intercept $\alpha(0) - 1 = 0$. In high energy proton–proton (pp) (and proton–antiproton, $p\bar{p}$) collisions, analysis of the experimental data showed that the total cross section grows approximately as follows (Donnachie and Landshoff 1992):

$$\sigma^{pp}_{tot} \sim s^{0.08}. \tag{3.22}$$

That is, using pre-QCD language, the pomeron intercept $\alpha_P - 1 = 0.08$. Since soft non-perturbative QCD physics is probably responsible for much of the total pp cross section observed at many modern-day accelerators, the pomeron with intercept $\alpha_P - 1 = 0.08$ is usually called the "soft pomeron".

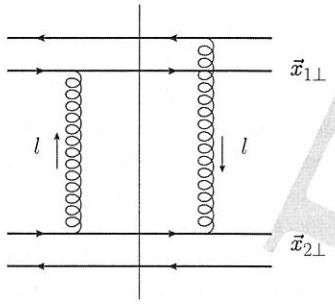

Fig. 3.4. A diagram contributing to the onium–onium high energy scattering cross section at leading order. The arrows next to the gluon lines indicate the direction of momentum flow and the vertical straight line denotes the final state cut.

We see that the prediction of Low and Nussinov that $\alpha_P - 1 = 0$, while it does not give the correct pomeron intercept, is not far from it, in the sense of giving a cross section that at least does not decrease with energy. (Of course there is no *a priori* reason to expect a perturbative calculation to describe the total pp scattering cross section, but it is good to have at least qualitative agreement between the two.) As we will see below, higher-order perturbative corrections to the cross section (3.18) generate a positive order-α_s contribution to the $\alpha_P - 1 = 0$ result. Note that the fact that experimental measurement of the total pp scattering cross section (3.22) gives a result that does not fall off with energy but instead rises slowly with s, when combined with the above rule for counting powers of s (see (3.6)), demonstrates that there must exist a spin-1 particle responsible for strong interactions – the gluon. This is exactly the argument for the existence of gluons mentioned in Sec. 1.1.

The $l_\perp$-integral in Eq. (3.18) has an infrared (IR) divergence. This is natural since we are calculating a cross section for the scattering of free color charges (quarks). To make the cross section IR-finite we need to remember that the scattering quarks are part of the onium wave functions. Suppose that the $q\bar{q}$ pairs have separations $\vec{x}_{1\perp}$ and $\vec{x}_{2\perp}$ in transverse coordinate space, though the impact parameter between the two onia has been integrated out. By summing diagrams with all possible gluon connections to quarks and antiquarks, one of which is shown in Fig. 3.4, one can then show that the total onium–onium scattering cross section is

$$\sigma_{tot}^{onium+onium} = \int d^2x_{1\perp} d^2x_{2\perp} \int_0^1 dz_1 dz_2 \, |\Psi(\vec{x}_{1\perp}, z_1)|^2 \, |\Psi(\vec{x}_{2\perp}, z_2)|^2 \hat{\sigma}_{tot}^{onium+onium} \quad (3.23)$$

with

$$\hat{\sigma}_{tot}^{onium+onium} = \frac{2\alpha_s^2 C_F}{N_c} \int \frac{d^2l_\perp}{(l_\perp^2)^2} \left(2 - e^{-i\vec{l}_\perp \cdot \vec{x}_{1\perp}} - e^{i\vec{l}_\perp \cdot \vec{x}_{1\perp}}\right)\left(2 - e^{-i\vec{l}_\perp \cdot \vec{x}_{2\perp}} - e^{i\vec{l}_\perp \cdot \vec{x}_{2\perp}}\right), \quad (3.24)$$

at the lowest order in α_s. Here $\Psi(\vec{x}_\perp, z)$ is the onium light cone wave function with quark light cone momentum fraction z. The exact form of the wave function is not important

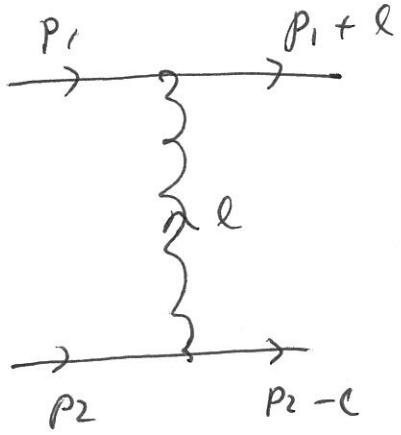

$$d\sigma = \frac{1}{2\cdot 2E_1\cdot 2E_2}\cdot\langle|M|^2\rangle\cdot\frac{d^2(p_1+\ell)_\perp\, d(p_1+\ell)^+}{(2\pi)^3\, 2(p_1+\ell)^+}$$

$$\cdot\frac{d^2(p_2-\ell)_\perp\, d(p_2-\ell)^-}{(2\pi)^3\, 2(p_2-\ell)^-}(2\pi)^4\cdot 2\cdot$$

$$\cdot\delta\big((p_1+\ell)^+ + (p_2-\ell)^+ - p_1^+ - p_2^+\big)\,\delta\big((p_1+\ell)^- + (p_2-\ell)^- - p_1^- - p_2^-\big)$$

$$\cdot\delta^2\big(p_1+\ell+p_2-\ell-p_1-p_2\big) = \Big|\ \text{as } p_1^\mu = (p_1^+, 0^-, \underline{0})\quad p_2^\mu = (0^+, p_2^-, \underline{0})$$

$$= \frac{1}{8E_1E_2}\langle|M|^2\rangle\frac{d^2\ell_\perp}{(2\pi)^2}\frac{1}{2p_1^+p_2^-} = \Big|\ s=(p_1+p_2)^2 = p_1^+p_2^-,\quad E_1 = p_1^+/2,\ E_2 = p_2^-/2$$

$$= \frac{1}{(2s)^2}\langle|M|^2\rangle\frac{d^2\ell_\perp}{(2\pi)^2}$$

$$\Rightarrow \boxed{d\sigma = \frac{1}{(2s)^2}\langle|M|^2\rangle\frac{d^2\ell_\perp}{(2\pi)^2}}$$

One can define $\boxed{A \equiv \frac{M}{2s}}$ rescaled amplitude, which is energy-independent for single gluon exchange. Then

$$\boxed{d\sigma = \langle|A|^2\rangle\frac{d^2\ell_\perp}{(2\pi)^2}}.$$

Example: Yukawa Potential

$$iM = (-ig)^2 \frac{i}{k^2 - m^2 + i\varepsilon} \bar{u}_{\sigma_1'}(p_1')\, u_{\sigma_1}(p_1)\, \bar{u}_{\sigma_2'}(p_2')\, u_{\sigma_2}(p_2)$$

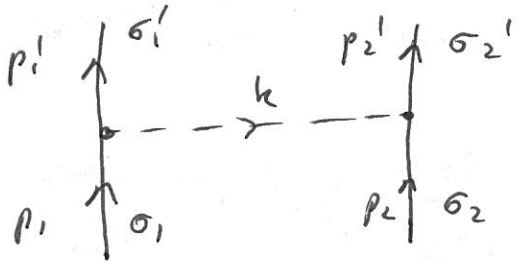

Assume protons are static & neglect recoil:

$$p_1'^{\mu} \simeq p_1^{\mu} = (M, \vec{0}) = p_2^{\mu} \simeq p_2'^{\mu}$$

$$\Rightarrow \bar{u}_{\sigma_1'}(p_1')\, u_{\sigma_1}(p_1) \simeq 2M \delta_{\sigma_1\sigma_1'}, \quad \bar{u}_{\sigma_2'}(p_2')\, u_{\sigma_2}(p_2) \simeq 2M \delta_{\sigma_2\sigma_2'}$$

Also, $p_1' = p_1 - k \Rightarrow (p_1')^2 = M^2 = (p_1 - k)^2 = M^2 + m_\pi^2 - 2M k^0$

$$\Rightarrow k^0 = \frac{m_\pi^2}{2M} \simeq 0 \Rightarrow k^2 = -\vec{k}^2.$$

$$iM = \underbrace{\frac{ig^2}{\vec{k}^2 + m_\pi^2}}_{-i\tilde{V}(\vec{k})} \cdot (2M)^2 \delta_{\sigma_1\sigma_1'} \delta_{\sigma_2\sigma_2'}$$

$$\Rightarrow \tilde{V}(\vec{k}) = \frac{-g^2}{\vec{k}^2 + m_\pi^2}$$

Potential between protons in momentum space.

$$V(r) = \int \frac{d^3k}{(2\pi)^3} e^{+i\vec{k}\cdot\vec{r}}\, \tilde{V}(\vec{k}) = \int \frac{d^3k}{(2\pi)^3} e^{i\vec{k}\cdot\vec{r}} \frac{-g^2}{\vec{k}^2 + m_\pi^2} =$$

$$= -\frac{g^2}{(2\pi)^2} \int_0^\infty \frac{dk \cdot k^2}{k^2 + m_\pi^2} \int_{-1}^{1} d\cos\theta\, e^{ikr\cos\theta} = \frac{ig^2}{(2\pi)^2} \frac{1}{r} \cdot \int_0^\infty \frac{dk \cdot k}{k^2 + m_\pi^2} \cdot$$

$$\cdot \left(e^{ikr} - e^{-ikr} \right) =$$

$$= \frac{ig^2}{(2\pi)^2}\frac{1}{r}\int_{-\infty}^{\infty}\frac{dk\cdot k}{k^2+m_\pi^2}e^{ik\cdot r} = \text{residues} =$$

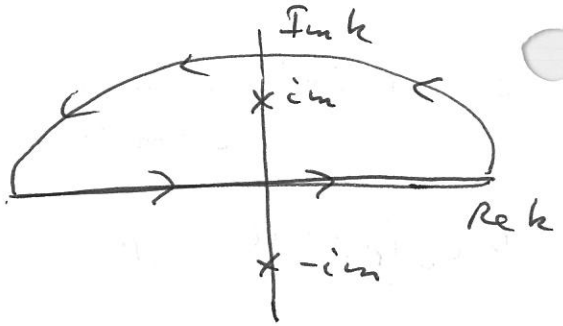

$$= \frac{ig^2}{(2\pi)^2}\frac{1}{r}\cdot(2\pi i)\frac{im_\pi}{2im_\pi}e^{-m_\pi r} =$$

$$= -\frac{g^2}{4\pi}\frac{e^{-m_\pi r}}{r}$$

$$\Rightarrow \boxed{V(r) = -\frac{g^2}{4\pi}\frac{e^{-m_\pi r}}{r}}$$

Yukawa potential

Yukawa: range of potential $\langle r\rangle \simeq \frac{1}{m_\pi}$

put $\langle r\rangle \simeq 1$ fm ~ internucleon distance

$\Rightarrow$ predicted a new particle (pion)

with mass $m \simeq \frac{1}{1\,\text{fm}} \simeq 200$ MeV

(not bad, as $m_\pi \approx 140$ MeV in reality).

$\Rightarrow$ the potential is <u>always</u> attractive:

$pp, pn, nn \ldots$